ORIGINAL ARTICLE

In Vivo Optical Coherence Tomography of the Human Oral Cavity and Oropharynx

James M. Ridgway, MD; William B. Armstrong, MD; Shuguang Guo, PhD; Usama Mahmood, MD; Jianping Su, BS; Ryan P. Jackson, ME; Terry Shibuya, MD; Roger L. Crumley, MD, MBA; Mai Gu, MD, PhD; Zhongping Chen, PhD; Brian J.-F. Wong, MD, PhD

Optical coherence tomography (OCT) is an evolving imaging modality that combines interferometry with low-coherence light to produce high-resolution tissue imaging. Cross-sectional in vivo images were obtained using an OCT device consisting of a Michelson interferometer, 1.3-μm broadband light source, and a handheld fiberoptic imaging probe. Image pixel resolution approached 10 μm. The mucosa of the oral cavity and oropharynx were examined in 41 patients during operative endoscopy. Optical coherence tomographic imaging was combined with endoscopic photography for gross and histologic image correlation. Optical coherence tomographic images of the oral cavity and oropharynx provided microanatomical information on the epithelium, basement membrane (BM), and supporting lamina propria (LP) of the mucosa. Normal microstructures identified in these tissues included an overlying keratin layer, papillae, ducts, glands, and blood vessels. Regions of pathologic features studied included mature scar, granulation tissue, mucous cysts, leukoplakia, and invasive cancer. Optical coherence tomographic imaging showed distinct zones of normal, altered, and ablated tissue microstructures for each pathologic process studied. Abnormal findings were directly compared with regions of normal tissue or conventional histopathologic features when tissue for analysis was available. This study provides a composite series of in vivo OCT images of the oral cavity and oropharynx in a variety of normal regions and pathologic states as well as outline future applications of OCT technology. *Arch Otolaryngol Head Neck Surg. 2006;132:1074-1081*

The National Cancer Institute estimates that newly diagnosed cancers of the oral cavity and pharynx affected 28 260 Americans and accounted for almost 7300 deaths in 2004.[1] Within the United States these malignant neoplasms constitute almost 3% of all cancers in men and 2% of all cancers in women.[2] Unfortunately, advances in surgery, radiotherapy, and chemotherapy have offered limited progress in terms of overall patient survival as regional failure and distant tumor recurrences continue to account for the disconcerting mortality rates over the last 2 decades.[3,4] The single greatest determinant of long-term patient survival remains early lesion detection and effective treatment. Presently, noninvasive imaging methods are unable to characterize the tissue microstructures in the epithelium and subepithelial layers. A reliable means to noninvasively image living tissues at high resolution could add substantially to the diagnosis, treatment, and monitoring of benign and malignant diseases within the upper aerodigestive tract.

Optical coherence tomography (OCT) is an emerging noninvasive, noncontact technology capable of high-resolution imaging of the mucosal epithelium and lamina propria (LP). Optical coherence tomography combines light from a low

Author Affiliations: Departments of Otolaryngology–Head and Neck Surgery (Drs Ridgway, Armstrong, Mahmood, Shibuya, Crumley, and Wong and Mr Jackson) and Pathology (Dr Gu), University of California Irvine, Orange; Beckman Laser Institute (Drs Ridgway, Guo, Mahmood, Chen, and Wong, and Messrs Jackson and Su) and Department of Biomedical Engineering, Rockwell Engineering Center (Drs Guo, Chen, and Wong, and Messrs Jackson and Su), University of California Irvine, Irvine.

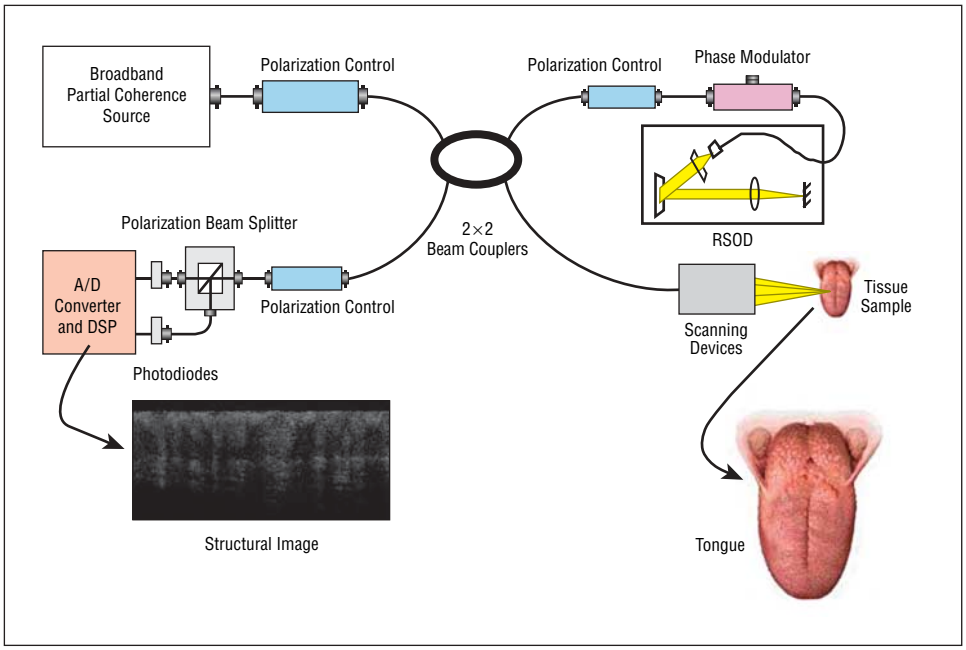

Figure 1. Schematic of optical coherence tomographic (OCT) imaging system and oral cavity/oropharynx target. The OCT system parameters are as follows: λ = 1310 nm and full width half maximum = 80 nm; lateral resolution = 15 μm; axial resolution = 10 μm; frame rate: 1 to 2 Hz. A/D means analog to digital conversion; DSP indicates digital signal processing; and RSOD, Rapid Scanning Optical Delayline.

coherence light source with a Michelson interferometer to produce cross-sectional images of tissue structures. Conceptually, OCT is analogous to B-mode ultrasonography but uses broadband near-infrared light, rather than sound energy, to produce images with a resolution approaching that of light microscopy (10-15 μm).[5,6] Optical coherence tomography images differences in the tissue optical properties, which includes the effects of both optical absorption and scattering. Tomographic systems are used in ophthalmology and dermatology, but in vivo study of OCT in the human oral cavity and oropharynx has been limited.[7,8]

In this study, we used a multipurpose OCT system for imaging the oral cavity and oropharynx during surgical endoscopy and in the clinical outpatient setting with the primary objectives of characterizing tissue microstructures and evaluating the efficacy of OCT to image the surface and submucosal tissues.

METHODS

PATIENTS

Optical coherence tomographic imaging was performed on patients undergoing oral examination in the outpatient clinic and during surgical endoscopy at the University of California Irvine Medical Center under protocol approved by the Human Subjects Institutional Review Board at the University of California Irvine, Orange. While the patient was under general anesthesia, OCT imaging was performed with a handheld probe positioned manually or with endoscopic guidance. Digital photographs of imaged areas were obtained and, when clinically indicated, correlative biopsy specimens were obtained.

OCT SYSTEM AND IMAGING

The components of our fiber-based OCT system are schematically illustrated in **Figure 1**. Near-infrared light from a broadband light source (central wavelength λ = 1310 nm, FWHM [full width at half maximum] Δλ = 80 nm, AFC BT 1310; JDS Uniphase, San Jose, Calif) enters a 2 × 2 fiber coupler. In the reference arm, a rapid scanning optical delay line attains A-scan at 500 Hz without phase modulation. A phase modulator generates 500-kHz phase modulation for heterodyne detection. Signals backscattered from the sample arm are obtained by phase-resolved processing with the interference fringes. The lateral and axial resolution of the system is approximately 10 μm per pixel. The horizontal image window was set laterally from 2 to 10 mm in length while detailed images of tissue microstructure were recorded up to a depth of 1.6 mm, depending on the turbidity of the media.

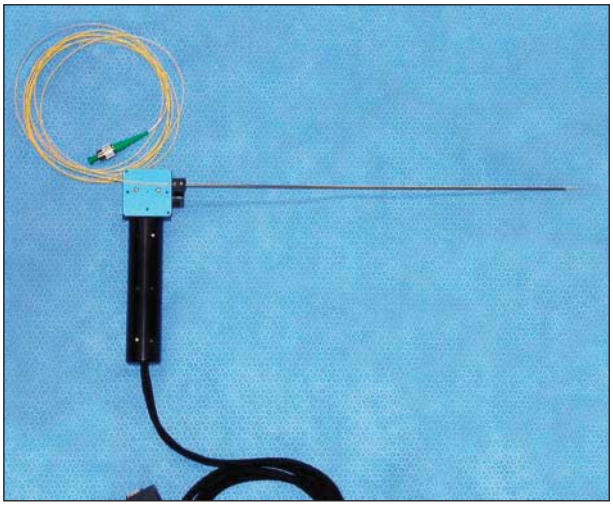

Figure 2. View of optical coherence tomographic handheld probe.

To image the oral cavity and oropharynx in vivo, a custom flexible OCT probe was designed to accommodate specific anatomical structures (**Figure 2**). The probe consists of a 900-μm, single-mode, 1310-nm OCT imaging fiber distally mounted with a gradient refractive index lens and a 0.7-mm right-angle prism (**Figure 3**). The gradient refractive index lens is 1.00 mm in diameter, has a 0.23 pitch, and works as a focuser. Mounting of the prism and gradient refractive index lens is performed with an optics grade, low-viscosity, wicking UV glue.

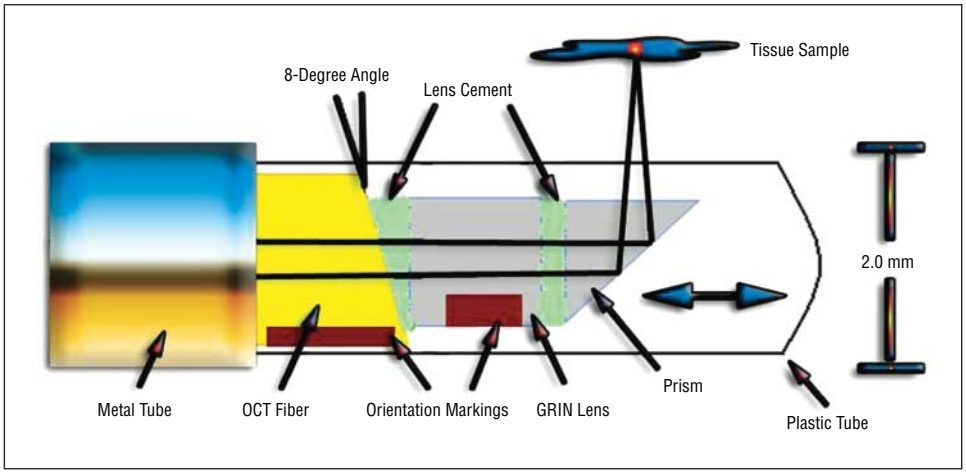

Figure 3. Optical coherence tomographic (OCT) probe tip depicting gradient refractive index (GRIN) lens and prism mounted at the end of the optic fiber.

Table 1. Number of Patients Imaged With Optical Coherence Tomography by Anatomical Regions and Subsites

Anatomical Regions	Locations Imaged	No. in Series
Oral cavity	Alveolar ridge	7
	Buccal mucosa	6
	Floor of mouth	16
	Gingiva	7
	Hard palate	3
	Lip (keratinized)	3
	Lip (mucosal)	6
	Tongue	11
	Tooth	3
	Uvula	2
Oropharynx	Base of tongue	15
	Palatine tonsil	5
	Posterior pharyngeal wall	2
	Soft palate	2
	Vallecula	2

Table 2. Number of Optical Coherence Tomographic Images With Benign and Malignant Processes in the Oral Cavity and Oropharynx Confirmed by Histologic Features

Diagnosis	Oral Cavity	Oropharynx	Total
Inflammation	4	7	**11**
Cyst	2	2	**4**
Acanthosis	1	0	**1**
Hyperplasia	0	1	**1**
Hyperkeratosis	2	1	**3**
Parakeratosis	3	1	**4**
Fibrosis	1	4	**5**
Granulation tissue	0	1	**1**
Metaplasia	0	1	**1**
Dysplasia	1	4	**5**
Leukoplakia	1	1	**2**
Ulceration	0	1	**1**
Carcinoma in situ	1	3	**4**
Verrucous carcinoma	4	1	**5**
Squamous cell carcinoma	14	6	**20**
Total	**34**	**34**	**68**

Scanning is achieved by linearly translating the fiber optic along the long axis using a motorized stage (model 663.4pr; PI Line, Tustin, Calif). The fiber optic and optical elements are enclosed by a transparent plastic tube (1.95-mm inner diameter, 0.21-mm thickness, fluorinated ethylene propylene material), which is mechanically supported and protected by a secondary outer stainless steel cylinder. To help orient the user, colored markings were made along the sides of the optic fiber and opposite light exit along the fiber tip.

The probe design was optimized during clinical evaluation to decrease bulk, improve acquisition speed, and optimize image quality. The current design was used for more than 95% of cases reported in this study. Image acquisition was monitored in real time on a 17-in LCD (liquid crystal display) monitor placed alongside the endoscopy video monitor. The entire OCT system is contained in a mobile endoscopy tower.

OCT IMAGE ANALYSIS

Images from multiple sites in the oral cavity and oropharynx were obtained. Acquired images were then sorted into the following 4 categories: normal healthy tissues, benign pathologic features (nonmalignant and precancerous lesions), invasive cancer, and transition zones at the borders of benign and malignant lesions. A breakdown of the images obtained at each anatomical site is tabulated in **Table 1** and **Table 2**.

HISTOLOGY

In cases in which biopsy specimens were obtained, histopathologic features were compared with OCT images to assess epithelial thickness, basement membrane (BM) integrity, and characterization of tissue microstructures within the LP. The OCT images were then used to construct a database of normative in vivo tissue microanatomy and pathology.

RESULTS

Forty-one adult subjects ranging in age from 24 to 89 years participated in an OCT study of the oral cavity and oropharynx. Optical coherence tomographic images were collected from multiple sites during operative endoscopy in 34 subjects and in the outpatient clinic in an additional 7 subjects. When clinically indicated, histologic biopsy specimens were obtained and compared with OCT images and lesion photographs. In cases in which no biopsy was indicated, comparison of OCT images was made using standard histologic criteria.[9-13] The distribution of images obtained is displayed in Table 1. Images were collected, and categorized, first separating normal anatomi-

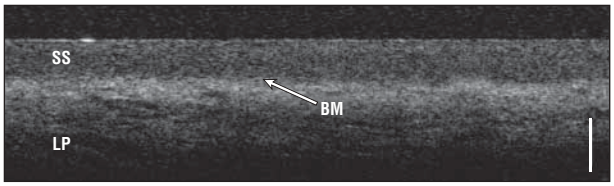

Figure 4. Optical coherence tomographic image of healthy buccal mucosa. BM indicates basement membrane; LP, lamina propria; SS, stratified squamous epithelium; and vertical bar, 500 µm.

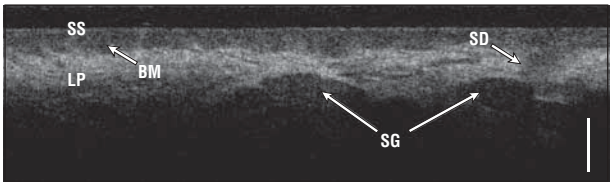

Figure 5. Optical coherence tomographic image of the mucosal side of the lower lip. BM indicates basement membrane; LP, lamina propria; SD, seromucinous duct (tangential slice); SG, seromucinous glands; SS, stratified squamous epithelium; and vertical bar, 500 µm.

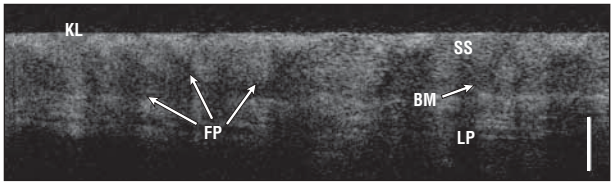

Figure 6. Optical coherence tomographic image of the dorsum of the tongue. BM indicates basement membrane; FP, filiform papillae; KL, keratin layer; LP, lamina propria; SS, stratified squamous epithelium; and vertical bar, 500 µm.

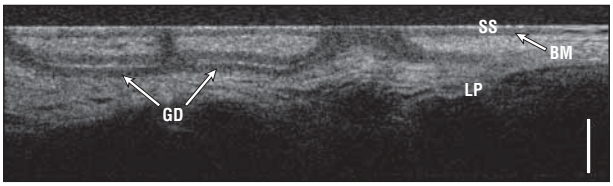

Figure 7. Optical coherence tomographic image along the floor of the mouth revealing extensive glandular duct (GD) system. BM indicates basement membrane; LP, lamina propria; SS, stratified squamous epithelium; and vertical bar, 500 µm.

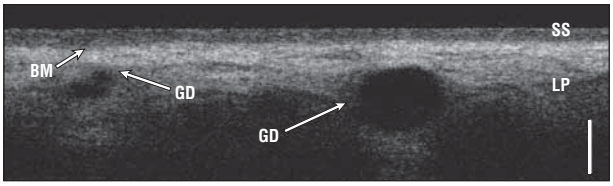

Figure 8. Optical coherence tomographic image along the undersurface of a healthy tongue. BM indicates basement membrane; GD, glandular duct; LP, lamina propria; SS, stratified squamous epithelium; and vertical bar, 500 µm.

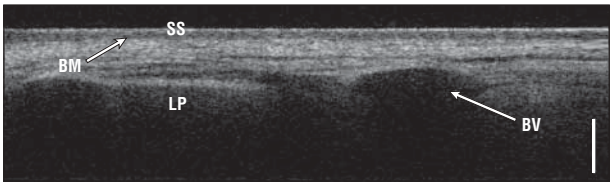

Figure 9. Optical coherence tomographic image of healthy floor of mouth with blood vessel imaging. BM indicates basement membrane; BV, blood vessel; LP, lamina propria; SS, stratified squamous epithelium; and vertical bar, 500 µm.

cal structures from pathologic lesions. Images from clinically evident pathologic lesions were subdivided into benign processes, premalignant lesions, and malignant lesions. Attention was also given to images demonstrating transitions from pathologic tissue changes and normal histopathology. Multiple benign and malignant pathologic lesions were identified, and are tabulated in Table 2.

The following tomographic series represents a survey of tissue imaging in which epithelium, BM, LP, and other regional microstructures were clearly identified in normal tissues using OCT (group 1). Each OCT image represents a specific region of interest with common and unique characteristics. **Figure 4** is a classic OCT image of normal buccal mucosa with clear identification of the stratified squamous epithelium (SS) along the mucosal surface, the underlying LP, and the transition between these tissues along BM boundary. The darker appearance of the epithelium is directly related to its lower optical density and scattering properties, which, in turn, results in lower signal intensity. By contrast, the LP is a more optically dense tissue and appears brighter in comparison caused by a higher signal intensity. Taking note of these optical differences, OCT permits identification of seromucinous glands along the mucosal surface of the lower lip (**Figure 5**), filiform papillae along the dorsum of the tongue (**Figure 6**), and the elaborate glandular duct system within the floor of the mouth (**Figure 7**). Signal propagation or absorption allowed for further characterization of tissue microstructures. Duct and lymphatic systems are characterized by regions of low signal intensity (black regions), which likely represent clear fluid that does not scatter or absorb light. As a result, signal intensity is relatively undiminished after passing through these structures and is readily observed beyond their distal walls (**Figure 8**). In contrast, blood vessels produce an "optical shadow" with the absorption of light by hemoglobin and the result of the image loss beyond the point of the proximal vessel lumen (**Figure 9**). The normal tissue OCT studies (group 1) provides a set of reference images for comparative analysis with diseased tissues (groups 2-4).

In group 2, tissue microstructure was different in comparison with native tissues depending on the pathophysiology. For example, in **Figure 10**, OCT images of a mucus-filled vallecular cyst show 2 thin tissue layers and a region of hyperplastic epithelium enveloping a large region of low signal intensity (presumably turbid mucus); correlative endoscopic and histologic images are provided for comparison. In other accounts, signal intensity and uniformity of regional epithelium was markedly different compared with group 1. As seen in **Figure 11**, OCT imaging of leukoplakia revealed increased optical density of the epithelium, superficial signal "flash points" with secondary shadow formation, and a varying epithelial thickness (Figure 11). These findings represented acanthosis, hyperkeratosis, mild dysplasia, and chronic inflammation in correlative histologic analysis.

In invasive malignant neoplasms (group 3), marked changes in the appearance of the OCT images were identified. Ablation of the tissue architecture and elimination of the BM were seen in all cases of histologically

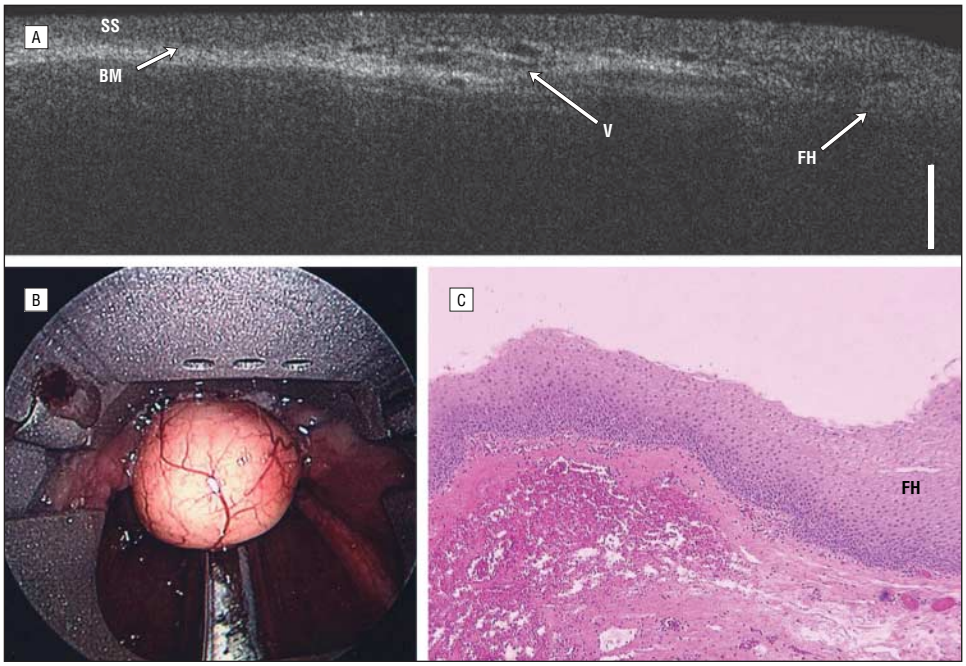

Figure 10. Multimodal analysis of a vallecular cyst using optical coherence tomography (A); endoscopic view (B), and correlative histologic features (C). BM indicates basement membrane; FH, follicular hyperplasia; SS, stratified squamous epithelium; V, vessels; and vertical bar, 500 µm.

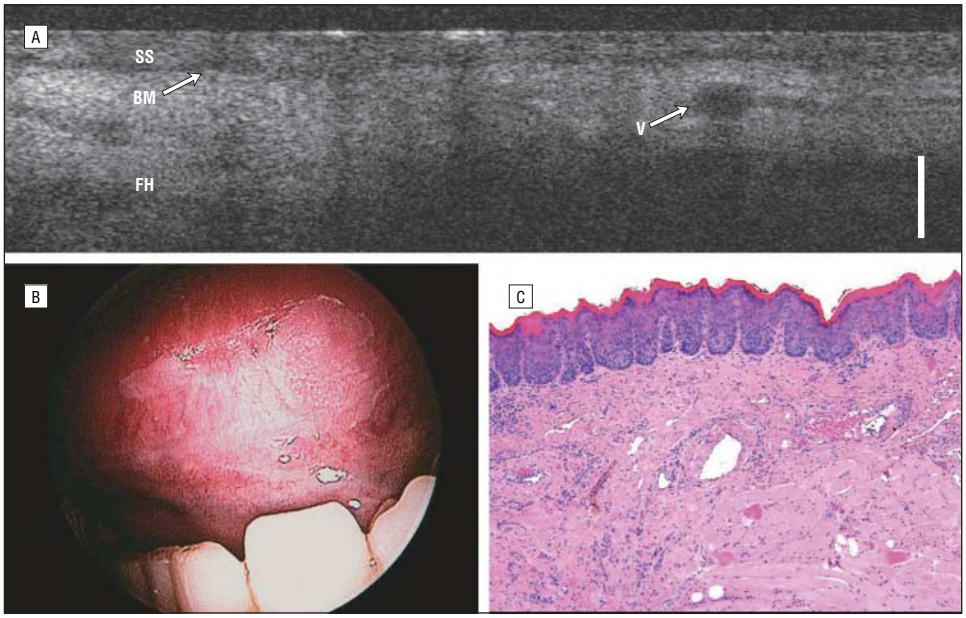

Figure 11. Imaging of region involving leukoplakia using optical coherence tomography (A); endoscopic view (B), and correlative histologic features (C). BM indicates basement membrane; LP, lamina propria; SS, stratified squamous epithelium; V, vessels; and vertical bar, 500 µm.

proven malignancy. **Figure 12** clearly demonstrates the characteristic loss of layering and BM integrity. Elimination of the BM in addition to the destruction of normative tissue microstructures produced images with poorly identifiable landmarks, boundaries, or microanatomical structures.

During the study, careful attention was made to image the clinical margins of both benign and malignant lesions (group 4). Disruption of tissue architecture was observed as pathologic tissues encroached into healthy regions. In **Figure 13**, the transition from normal epithelium and BM to invasive tumor is clearly demonstrated. Furthermore, tangential orientation of OCT imaging along the boundary of a lesion revealed multiple points of BM invasion offset by islands of intact microarchitecture (**Figure 14**).

The histologic images shown in Figures 10 through 14 illustrate the submucosal microanatomy for each of the related OCT Images. These histologic cross sections correlate with the OCT cross-sectional images, confirming the findings noted above.

COMMENT

The in vivo characterization of mucosal and submucosal tissues is of exceptional value in the treatment, diagnosis, and monitoring of both benign and malignant diseases within the upper aerodigestive tract. The tissues of the oral cavity and oropharynx are readily accessible with epithelial changes observed long before BM transgression in premalignant conditions. Unfortunately, considerable chal-

lenges exist in distinguishing premalignant lesions from early tumor development on physical inspection and with current noninvasive modalities. Characterization of pathologic lesions is limited by the inability to look into the tissues. Visual imaging provides information about the surface of the lesion but very limited information about the BM and subsurface structures.

Within the oral cavity and oropharynx healthy epithelium varies from 75 to 550 µm in thickness while the underlying the LP may extend up to 2000 µm.[12,13] To reliably characterize mucosal pathologic processes an imaging modality must have a functional resolution approaching 10 µm.[14] In comparison, the effective resolutions of magnetic resonance imaging (0.5-1 mm), computed tomography (0.5-1 mm), positron emission tomography (1-5 mm), and ultrasonography (100-500 µm) are at least an order of magnitude larger than required to observe pathologic changes in the boundary between the epithelium and the LP.[15-17] Other modalities, such as contact endoscopy, use in vivo staining with methylene blue, acetic acid, or indigo carmine to produce a resolution of 10 to 71 µm with the capability of observation up to 100 µm below the tissue surface.[18] Only the most superficial layers of the epithelium can be visualized due to intrinsic optical limitations, and the images are obtained in an en face plane, an orientation that clinicians trained in reading cross-sectional histology are unaccustomed to. Furthermore, many disease processes of the oral mucosa result in immense epithelium thickening, thereby precluding any possibility of BM evaluation using existing technology.[14,19] As a result of these limitations, tissue biopsy remains the diagnostic procedure of choice.

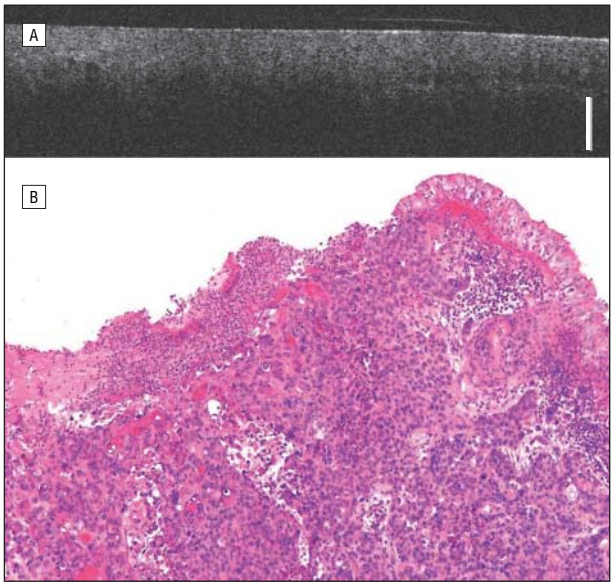

Figure 12. Invasive squamous cell carcinoma of maxilla illustrated using optical coherence tomography (A) and correlative histologic features (B). Note absence of basement membrane and tissue microstructures. Vertical bar indicates 500 µm.

Optical coherence tomographic imaging can produce detailed cross-sectional images of the subsurface microstructure at an axial resolution of approximately 9 µm and a lateral resolution of 10 µm using safe low-power near infrared light in vivo and in real time. Optical coherence tomography has been used in ophthalmology,[20-22] but its use in the head and neck has been limited, as imaging requires the patient to remain motionless and endoscopy is often needed to visualize the region of interest. Because of the combined requirement for the patients to remain motionless and the need for general anesthesia in most head and neck endoscopy, most studies to date have focused on the ex vivo imaging of analogous animal tissues.[7,8,23-25] Ex vivo tissue has considerably different optical properties than in vivo due to the loss of blood, oxidation of hemoglobin, and tissue desiccation. In the head and neck, only a few limited in vivo imaging studies have been published that have focused on patients with cancer. Sergeev et al[26] and Bouma and Tearney[27] have reported the use of

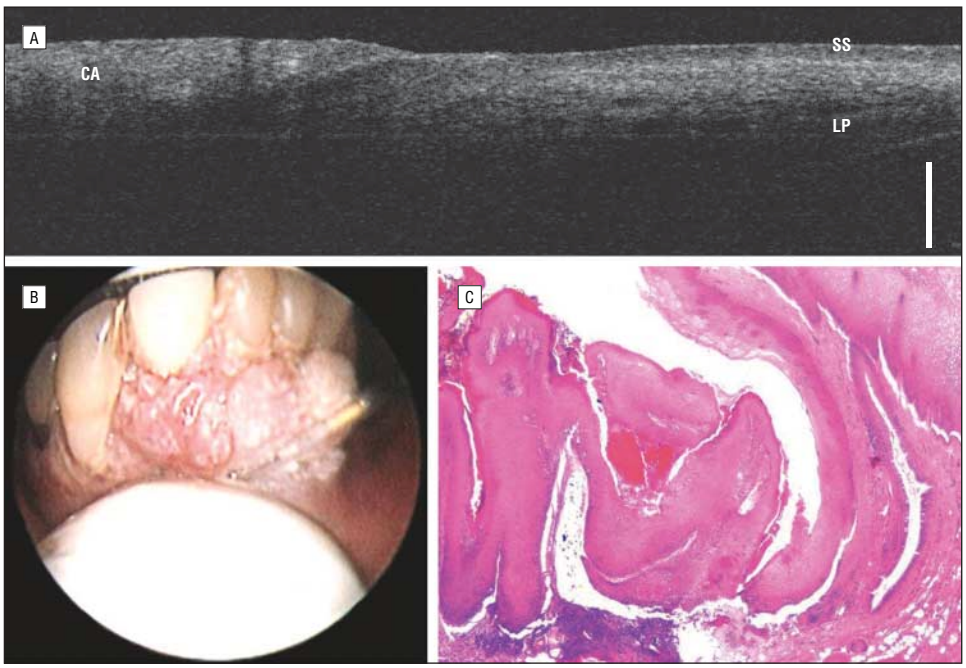

Figure 13. Multimodal analysis revealing transition zone of cancer and adjacent tissue along anterior mandible margin using optical coherence tomography (A); endoscopic view (B), and correlative histologic features (C). CA indicates cancer (squamous cell carcinoma); LP, lamina propria; SS, stratified squamous epithelium; and vertical bar, 500 µm.

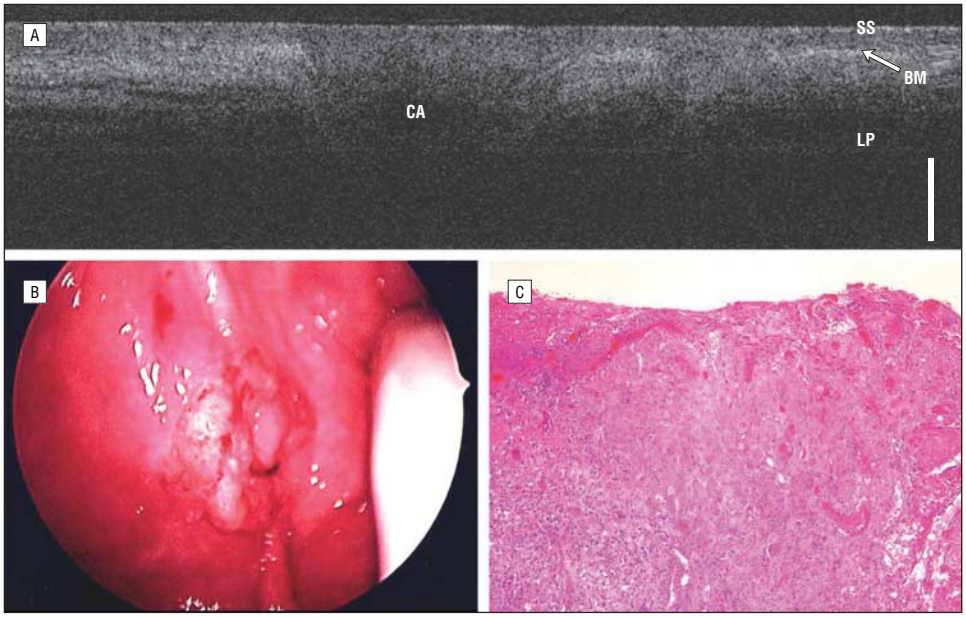

Figure 14. Imaging of cancer transition zones and adjacent tissues along alveolar border using optical coherence tomography (A); endoscopic view (B), and correlative histologic features (C). BM indicates basement membrane; CA, cancer (squamous cell carcinoma); LP, lamina propria; SS, stratified squamous epithelium; and vertical bar, 500 µm.

OCT in the aerodigestive tract. These findings were limited by the challenges in the depth of imaging, resolution, and speed of image acquisition inherent in OCT imaging. By using a different light source and a faster and more robust piezoelectric translation stage, we have been able to improve resolution from 15 to 20 µm to 10 µm, increase maximum image depth by almost 50%, vary the horizontal image width from 2 mm to up to 10 mm, and increase the frame capture rate from 1.5 to 2 seconds for a 2-mm scan to 1 second for a 6-mm scan. The improved resolution and depth of imaging allows more rapid and precise characterization of the tissue structures, which we have used to perform extensive in vivo imaging of normal, benign, and malignant tissues in the oral cavity and oropharynx.

This study confirms the feasibility of using OCT to identify differences in mucosal and submucosal tissue structures of the oral cavity and oropharynx. Epithelium, LP, and BM boundaries were clearly identified in all normal tissues imaged. Each tissue microstructure, including papillae, glands, ducts, and blood vessels, revealed unique optical characteristics that allowed for image correlation with known histologic features. Optical coherence tomographic imaging of pathologic conditions such as leukoplakia revealed benign changes in epithelial density and tissue thickness without alteration in the BM. In contrast, OCT images of early cancer revealed ablation of normal tissue microanatomy in addition to BM compromise. Further imaging of lesion borders revealed transition zones between cancerous and noncancerous tissues. Optical coherence tomographic images of these clinically suspicious lesions were correlated with histologic specimens and intraoperative digital photographs. Of particular note were the considerable histologic distortions created by tissue biopsy as well as fixation of specimens when compared with OCT images of the same region. The in vivo OCT imaging of living tissues may represent a truer biologic picture than any image produced by other high-resolution modalities.

The ability to perform in vivo tissue imaging with a noninvasive, high-resolution modality could significantly alter the detection and management of early stage disease. With the capability to perform a tomographic study, one could easily monitor disease, document progression, and target tissue biopsy specimens to regions of greater histologic yield. Additionally, OCT is an evolving imaging modality where both improvements in source coherence bandwidth and electromechanical design will lead to higher-resolution images and faster frame rates.

The application of this high-resolution imaging modality provides valuable information on the physiology of benign mucosal disorders and on the development, transformation, and progression of cancer. Our ongoing OCT investigations are focused on new applications in children, microsurgery, and office-based instruments, in addition to continuing to expand our adult clinical series.

Submitted for Publication: May 3, 2005; final revision received March 12, 2006; accepted April 22, 2006.
Correspondence: Brian J.-F. Wong, MD, PhD, or Zhongping Chen, PhD, Beckman Laser Institute and Medical Clinic, University of California, Irvine, 1002 Health Sciences Rd, East Irvine, CA 92617 (bjwong@uci.edu or z2chen@uci.edu).
Author Contributions: Drs Ridgway, Jackson, Crumley, and Wong had full access to all the data in the study and take responsibility for the integrity of the data and the accuracy of the data analysis. *Study concept and design:* Ridgway, Jackson, Guo, Armstrong, Crumley, Chen, and Wong. *Acquisition of data:* Ridgway, Guo, Mahmood, Su, Armstrong, Shibuya, Crumley, Chen, and Wong. *Analysis and interpretation of data:* Ridgway, Armstrong, Crumley, Gu, and Wong. *Drafting of the manuscript:* Ridgway, Su, Armstrong, and Wong. *Critical revision of the manuscript for important intellectual content*: Ridgway, Jackson, Guo, Mahmood, Armstrong, Shibuya, Crumley, Gu, Chen, and Wong. *Statistical analysis:* Ridgway. *Obtained funding:* Wong. *Administrative, technical, and ma-*

terial support: Ridgway, Jackson, Guo, Mahmood, Su, Armstrong, Shibuya, Gu, and Wong. *Study supervision:* Armstrong, Crumley, Chen, and Wong.

Financial Disclosure: None reported.

Funding/Support: This study was supported by grants DC 006026, CA 91717, EB 00293, RR 01192, and M01-RR00827-28 from the National Institutes of Health, grant 32456 from the Flight Attendant Medical Research Institute, grant 12RT-0113 from the State of California Tobacco Related Disease Research Program, and grant F49620-00-1-0371 from the Air Force Office of Scientific Research, and the Arnold and Mabel Beckman Foundation.

Previous Presentation: This study was presented in part at the annual meeting of the American Head and Neck Society; May 15, 2005; Boca Raton, Fla.

Acknowledgment: We thank master machinist Rudolph Limberg and Steve Knisley for assistance with construction of the instrument and Aya Yamamoto, RN, and Clevan Barclay, ST, for their help and patience in the operating room.

REFERENCES

1. American Cancer Society. *Cancer Facts and Figures 2004*. Oakland: California Division Inc; 2005.
2. National Cancer Institute. SEER Cancer Statistics Review 1975-2001. http://www.seer.cancer.gov. Accessed March 4, 2005.
3. Malone JP, Stephens JA, Grecula JC, Rhoades CA, Ghaheri BA, Schuller DE. Disease control, survival, and functional outcome after multimodal treatment for advanced-stage tongue base cancer. *Head Neck*. 2004;26:561-572.
4. Duvvuri U, Simental AA Jr, D'Angelo G, et al. Elective neck dissection and survival in patients with squamous cell carcinoma of the oral cavity and oropharynx. *Laryngoscope*. 2004;114:2228-2234.
5. Huang D, Swanson EA, Lin CP, et al. Optical coherence tomography. *Science*. 1991;254:1178.
6. Brezinski ME, Tearney GJ, Boppart SA, Swanson EA, Southern JF, Fujimoto JG. Optical biopsy with optical coherence tomography: feasibility for surgical diagnostics. *J Surg Res*. 1997;71:32-40.
7. Fomina IuV, Gladkova ND, Leont'ev VK, et al. Optical coherence tomography in the evaluation of the oral cavity mucosa, part II: benign and malignant diseases. *Stomatologiia (Mosk)*. 2004;83:25-32.
8. Gladkova ND, Shakhova NM, Shakhov BE, et al. Optic coherent tomography: a new high-resolution technology of visualization of tissue structures, part 1: principle of the technique: objects of OCT applications and technical decisions for their study. *Vestn Rentgenol Radiol*. March-April 2002:39-47.
9. Sternberg SS. *Histology for Pathologists*. New York, NY: Raven Press; 1992.
10. Eroschenko VP. *Atlas of Histology With Functional Correlations*. 9th ed. Philadelphia, Pa: Lippincott Williams & Wilkins; 2000.
11. Gartner LP, Hiatt JL. *Color Atlas of Histology*. 3rd ed. Philadelphia, Pa: Lippincott Williams & Wilkins; 2000.
12. Klein-Szanto AJ, Schroeder HE. Architecture and density of the connective tissue papillae of the human oral mucosa. *J Anat*. 1977;123:93-109.
13. Paulsen F, Thale A. Epithelial-connective tissue boundary in the oral part of the human soft palate. *J Anat*. 1998;193:457-467.
14. Andrea M, Dias O. *Atlas of Rigid and Contact Endoscopy in Microlaryngeal Surgery*. Philadelphia, Pa: Lippincott-Raven Publishers; 1995.
15. Black PM, Moriarty T, Alexander E, et al. Development and implementation of intraoperative magnetic resonance imaging and its neurosurgical applications. *Neurosurgery*. 1997;41:831-842.
16. Goldberg BB, Liu JB, Merton DA, et al. Sonographically guided laparoscopy and mediastinoscopy using miniature catheter-based transducers. *J Ultrasound Med*. 1993;12:49-54.
17. Andrew ER. Nuclear magnetic resonance and the brain. *Brain Topogr*. 1992;5:129-133.
18. Nelson DB, Block KP, Bosco JJ, et al. Technology status evaluation report: high-resolution and high-magnification endoscopy. *Gastrointest Endosc*. 2000;52:864-866.
19. Shakhov AV, Terentjeva AB, Kamensky VA, et al. Optical coherence tomography monitoring for laser surgery of laryngeal carcinoma. *J Surg Oncol*. 2001;77:253-258.
20. Rogers AH, Martidis A, Greenberg PB, Puliafito CA. Optical coherence tomography findings following photodynamic therapy of choroidal neovascularization. *Am J Ophthalmol*. 2002;134:566-576.
21. Ko TH, Fujimoto JG, Duker JS, et al. Comparison of ultrahigh- and standard-resolution optical coherence tomography for imaging macular hole pathology and repair. *Ophthalmology*. 2004;111:2033-2043.
22. Voo I, Mavrofrides EC, Puliafito CA. Clinical applications of optical coherence tomography for the diagnosis and management of macular diseases. *Ophthalmol Clin North Am*. 2004;17:21-31.
23. Wilder-Smith P, Jung WG, Brenner M, et al. In vivo optical coherence tomography for the diagnosis of oral malignancy. *Lasers Surg Med*. 2004;35:269-275.
24. Boppart SA, Brezinski ME, Fujimoto JG. Optical coherence tomography imaging in developmental biology. *Methods Mol Biol*. 2000;135:217-233.
25. Hanna N, Saltzman D, Mukai D, et al. Two-dimensional and 3-dimensional optical coherence tomographic imaging of the airway, lung, and pleura. *J Thorac Cardiovasc Surg*. 2005;129:615-622.
26. Sergeev AM, Gelikonov VM, Gelikonov GV, Feldchtein FI, Kuranov RV, Gladkova ND. In vivo endoscopic OCT imaging of precancer and cancer states of human mucosa. *Optic Express V1*. 1997;13:432-440.
27. Bouma BE, Tearney GJ. *OCT Handbook*. New York, NY: Marcel Dekker Inc; 2003:705-724.